Volume collapse in LaMnO$_3$ caused by an orbital order-disorder transition

Tapan Chatterji,[1,2] François Fauth,[3] Bachir Ouladdiaf,[1] P. Mandal,[4] and B. Ghosh[4]

[1]*Institut Laue-Langevin, BP 156, 38042 Grenoble Cedex 9, France*
[2]*Max-Planck-Institut für Physik Komplexer Systeme, Dresden, Germany*
[3]*European Synchrotron Radiation Research Facility, BP 220, 38043 Grenoble Cedex, France*
[4]*Saha Institute of Nuclear Physics, 1/AF Bidhannagar, Calcutta 700 064, India*

We have investigated the Jahn-Teller transition accompanied by the orbital order-disorder transition in LaMnO$_3$ by high temperature x-ray powder diffraction with synchrotron radiation and also neutron powder diffraction. The unit cell volume of LaMnO$_3$ decreases with increasing temperature in a narrow temperature range below $T_{JT} \approx 750$ K, and then undergoes a volume collapse at T_{JT}. We interpret this effect as due to the more efficient packing of the MnO$_6$ octahedra in the orbitally disordered or orbital liquid state. The orbital melting phenomenon can be qualitatively compared with the melting of ice.

PACS number(s): 61.12.Ld, 61.66.Fn

The parent compound LaMnO$_3$ of the hole-doped colossal magnetoresistance materials La$_{1-x}$A$_x$ MnO$_3$ (A = Ca, Sr, Ba) has attracted much interest from condensed matter scientists.[1,2] Stoichiometric LaMnO$_3$, in which Mn ions are formally Mn^{3+}, has an antiferromagnetic insulating ground state. Cooperative Jahn-Teller distortion removes the degeneracy of the e_g orbitals in the $t_{2g}^3 e_g^1$ electron configuration of the Mn^{3+} ions, and stabilizes $d_{3x^2-r^2}/d_{3y^2-r^2}$ orbitals which are ordered. The orbital order consists of the ordering of the $d_{3x^2-r^2}$ and $d_{3y^2-r^2}$ orbitals in an alternate staggered pattern (Fig. 1) in the a-b plane. The orbital ordering pattern repeats itself along the c axis. This type of orbital order induces A-type antiferromagnetic (AF) ordering[3,4] below $T_N \approx 140$ K. In the A-type AF phase the spins in the a-b plane are ferromagnetically ordered. The ferromagnetic planes are stacked antiferromagnetically along the c axis. The orbital order persists in the paramagnetic phase above T_N. A complete understanding of the mechanism stabilizing the observed order in the insulating parent compound LaMnO$_3$ is a prerequisite to understanding fully the complex interplay among the spin, charge, orbital, and lattice degrees of freedom in the doped manganites. For this reason a large number of theoretical investigations has already been undertaken on stoichiometric LaMnO$_3$ itself.[5] LaMnO$_3$ crystallizes in the orthorhombic space group *Pbnm* (Fig. 1). The MnO$_6$ octahedra in LaMnO$_3$ are distorted due to the Jahn-Teller effects. There are three Mn-O distances called short s, medium m, and long l. LaMnO$_3$ undergoes a transition at $T_{JT} \approx 750$ K from the Jahn-Teller distorted orthorhombic phase to a high temperature orthorhombic phase which is nearly cubic.[6] The space group *Pbnm* remains the same in both phases, but the Jahn-Teller distortion is nearly removed in the high temperature phase. The transition is accompanied by an orbital order-disorder transition. Abrupt changes in the electrical resistivity, thermoelectric power, and Weiss constant[7] have also been observed at this transition. During the present investigation we discovered an unusual abrupt volume contraction at $T_{JT} \approx 750$ K. The high temperature phase just above T_{JT} has less volume than the low temperature phase.

This volume contraction is very rare in solid-solid structural phase transition. A well-known example is the volume contraction in Fe (Ref. 8) at the bcc-to-fcc (α-Fe to γ-Fe) structural transition at $T_c \approx 1185$ K. However, this volume contraction in Fe is due to the transition from the relatively open bcc structure to the closed packed fcc structure. The volume contraction is known at the melting transition in hydrogen-bonded hexagonal ice[9] and the covalent tetrahedrally bonded Si and Ge,[10] and also in Bi, Ga, Ce and Pu.[10] However, to our knowledge no volume contraction has so far been reported at a Jahn-Teller transition.

High temperature x-ray powder diffraction experiments were done on the high resolution powder diffractometer at the undulator beam line ID31 of the European Synchrotron Radiation Facility in Grenoble. The x-ray wavelength was 0.495754 ± 0.00005 Å. In addition we have done high temperature neutron diffraction measurements[11] on the high resolution powder diffractometer D2B of the Institut-Laue-Langevin in Grenoble. Figure 2 shows the x-ray diffraction diagram of the high temperature phase LaMnO$_3$ at $T = 823$ K. The inset shows parts of the diffraction patterns at several temperatures showing the diffraction peaks of the low temperature and high temperature phases and their temperature dependence.

Figure 3 shows the temperature variation of the lattice parameters a, b, and $c/\sqrt{2}$ determined by x-ray diffraction. This variation is similar to that determined previously by neutron diffraction,[11] but the lattice parameters have been measured by x-ray diffraction in much finer temperature intervals close to T_{JT}. The lattice parameter b decreases and the parameters a and $c/\sqrt{2}$ increase with temperature and then abruptly become almost the same (metrically almost cubic) at T_{JT}. The transition is clearly first order, because in a temperature range of about 10 K both high and low temperature phases coexist. Figure 4(a) shows the temperature variation of the unit cell volume V of LaMnO$_3$, which increases linearly as a function of temperature from room temperature to about 600 K, and deviates from this linear behavior at higher temperatures. It shows a local maximum at about $T = 720$ K, then decreases with increasing temperature, and finally drops abruptly at $T_{JT} \approx 750$ K with a volume contraction of about 0.36% at T_{JT}. At higher temperature V increases linearly again with increasing temperature. Figure
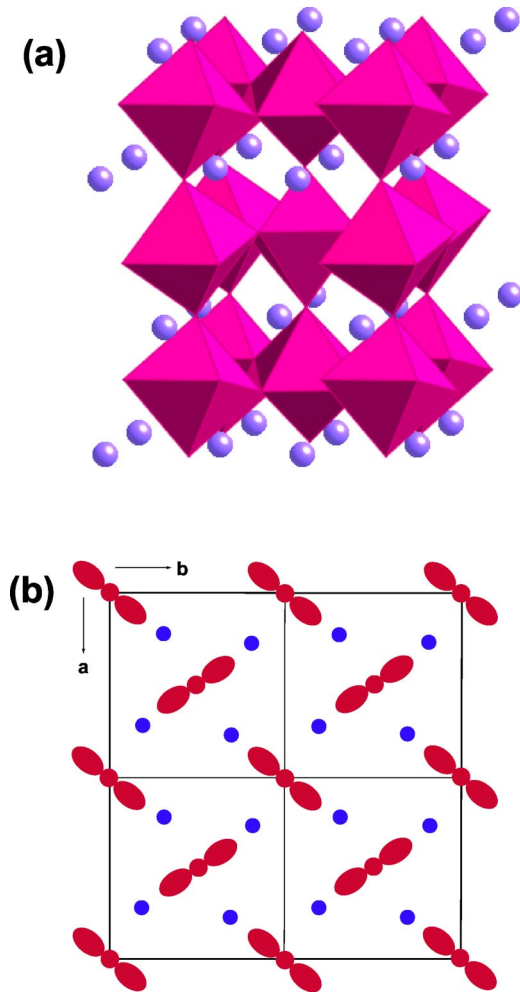
FIG. 1. (Color online) (a) Schematic representation of the ortho-rhombic crystal structure of LaMnO$_3$ in which only the La ions and the MnO$_6$ octahedra are shown. (b) The staggered ordering of the $d_{3x^2-r^2}$ and $d_{3y^2-r^2}$ orbitals in the a-b plane. The orbital ordering pattern is repeated along the c axis.
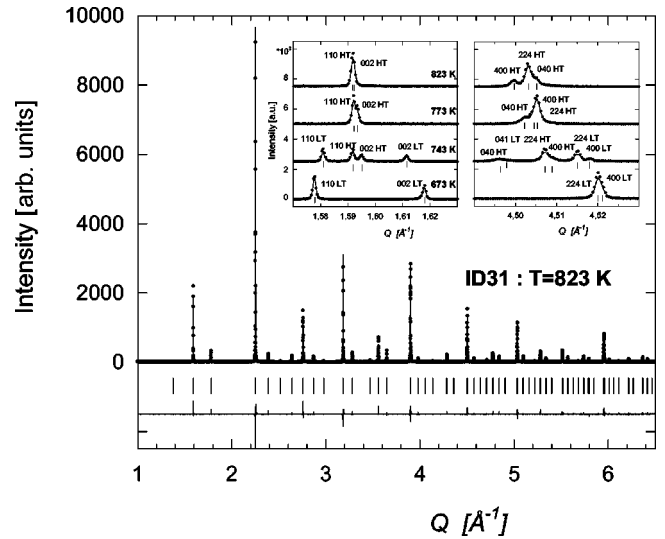

FIG. 2. X-ray diffraction diagram of LaMnO$_3$ at $T=823$ K. The inset shows parts of the diffraction patterns at several temperatures showing the diffraction peaks of the low temperature (LT or O') and high temperature (HT or O) phases and their temperature dependence.

4(b) shows the temperature variation of ΔV which is obtained from V after subtracting the cell volume ("base volume") obtained by the linear fit of the high temperature data. The temperature variation of this extra volume ΔV looks like an order parameter that decreases continuously at first and then drops abruptly to zero ("base volume") at T_{JT}.

High resolution x-ray diffraction from LaMnO$_3$ gave very accurate lattice parameters and unit cell volume. However, x-ray diffraction is not as sensitive as neutron diffraction for determining the positional parameters, particularly those of O atoms. We performed high temperature neutron powder diffraction measurements at a few selected temperatures to determine positional and thermal parameters of La, Mn, and O atoms from Rietveld refinements. The distortion of the MnO$_6$ octahedron due to the Jahn-Teller effect produces three Mn-O bond distances: long (l), short (s), and medium (m). The distorted crystal structure can be obtained from the ideal perovskite structure in the following way: first the distortion Q_2 of the octahedron formed with O^{-2} ions is added in a staggered way along the three directions,

and then the distortion Q_3 is superimposed on it. These two distortion modes are expressed in terms of l,s, and m by

$$Q_2=\frac{2}{\sqrt{2}}(l-s), \quad Q_3=\frac{2}{\sqrt{6}}(2m-l-s). \tag{1}$$

The distortion parameter Δ of an N-coordination polyhedron BO$_N$ with an average B-O distance $\langle d\rangle$ is defined as

$$\Delta=\frac{1}{N}\sum_{n=1,N}\left\{\frac{d_n-\langle d\rangle}{\langle d\rangle}\right\}^2. \tag{2}$$

Figure 5(a) shows the temperature dependence of the short s, long l, and medium m Mn-O bond distances determined from neutron diffraction data. Figure 5(b) shows the temperature
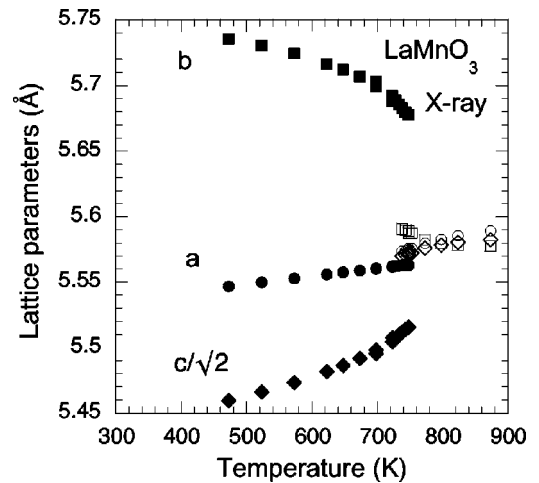

FIG. 3. Temperature variation of the lattice parameters of LaMnO$_3$. The error bars are smaller than the sizes of the data symbols.
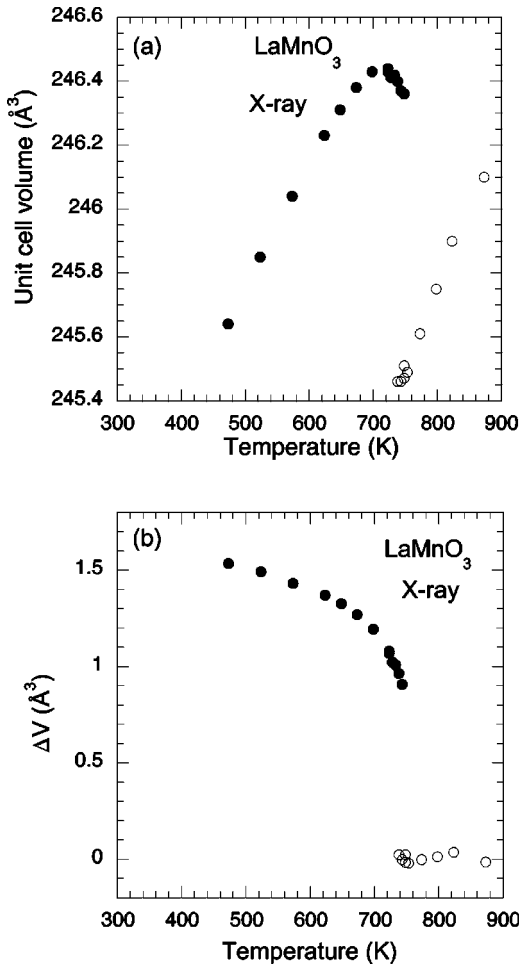
FIG. 4. (a) Temperature variation of the unit cell volume of LaMnO$_3$. (b) Temperature variation of the unit cell volume after subtraction of the base volume explained in the text.

dependence of the two distortion modes Q_2 and Q_3. Figure 5(c) gives the temperature dependence of the distortion parameter Δ. The average Mn-O bond distance $\langle d \rangle$ shows an abrupt contraction of about 0.45% at T_{JT}. The thermal parameters of all atoms increase as a function of temperature. However, the thermal parameters of the O atom become very large in the high temperature orthorhombic O and the rhombohedral R phases.

We heated the sample several times above T_{JT} and cooled down to room temperature during both x-ray and neutron diffraction investigations. The diffraction diagrams from the sample at room temperature were found to be identical to the original diagram each time and also the structural refinement gave identical results. This confirms that the observed volume collapse in LaMnO$_3$ is intrinsic, and is not due for example to the oxygen loss or other chemical changes.

Sánchez *et al.*[12] measured the heat capacity anomaly of LaMnO$_3$ at T_{JT}. The enthalpy involved in this transition is found to be $\Delta H = 3180 \pm 100$ J mole^{-1}. This value of ΔH combined with the volume drop at T_{JT} $\Delta V = -0.1535$ cm^3 mole^{-1} determined during the present investigation yields from the Clapeyron equation $\Delta T/\Delta P =$
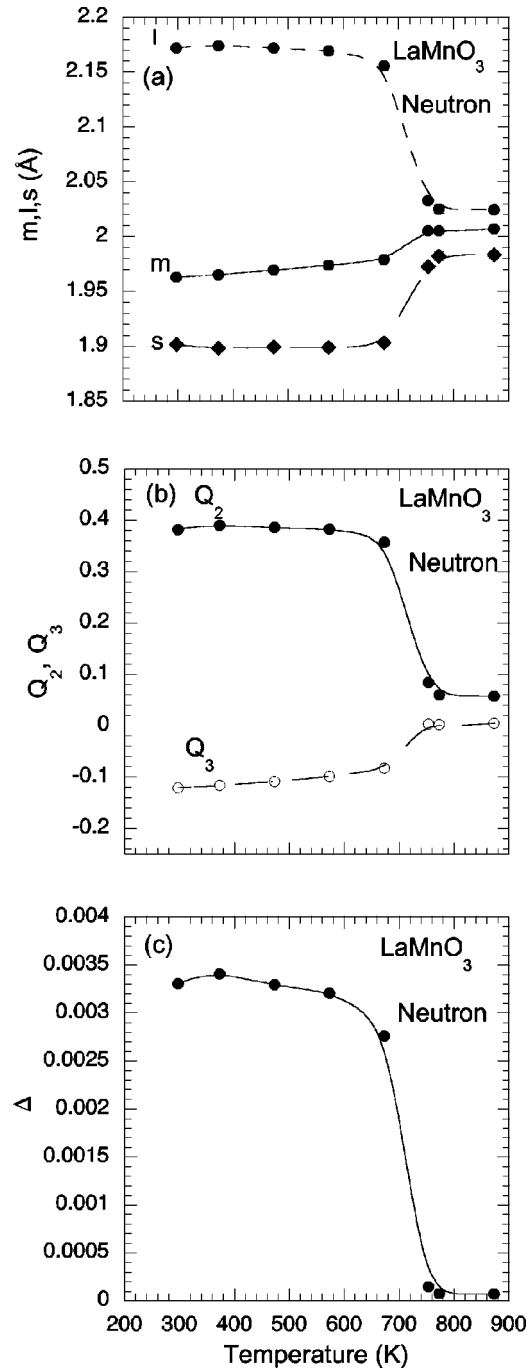

FIG. 5. (a) Temperature variation of the three Mn-O bond lengths m, l, and s of LaMnO$_3$. (b) Temperature variation of the two octahedral distortion modes, Q_2 and Q_3 defined in Eq. (1). (c) Temperature variation of the distortion parameter defined in Eq. (2). The smoothed curves are guide to the eyes.

-3.62 K kbar^{-1}. By simple extrapolation T_{JT} in LaMnO$_3$ can be brought down to room temperature by the application of pressure of about 125.7 kbar or 12.57 GPa. Loa *et al.*[13] performed high pressure x-ray diffraction on LaMnO$_3$ and they conclude that Jahn-Teller distortion in LaMnO$_3$ is removed at room temperature by the application of pressure of about 180 kbar. Sánchez *et al.*[12] interpreted the transition at T_{JT} as an order-disorder transition where the statistical occu-
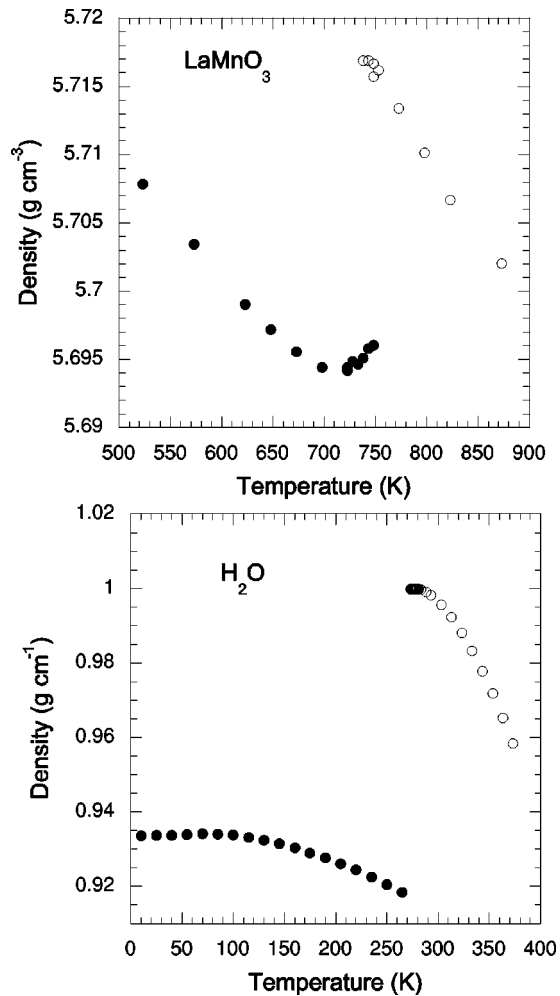
FIG. 6. (a) Temperature variation of the density of LaMnO$_3$ close to T_{JT}. (b) Temperature variation of the density of ice close to the ice melting.

pation in the disordered phase corresponds to the three possible orientations of the tetragonal distortions on each octahedron. They claimed that the three-state Potts model is the appropriate statistical model for this transition. However, the

calculated value of entropy at T_{JT} does not agree with the experimental value.

The negative thermal expansion in a narrow temperature range and the abrupt volume contraction at T_{JT} in LaMnO$_3$ are connected with the orbital order-disorder transition. The orbitally disordered state allows a more efficient packing of the MnO$_6$ octahedra. The situation can be compared with the volume reduction as ice melts into water. The orbitally ordered state with Jahn-Teller distorted octahedra requires more volume like the directionally ordered hydrogen bonds in ice. However, orbital melting is essentially an electronic phenomenon whereas ice melting is a melting of the crystal lattice. The enthalpy change at the melting of ice[14] is $\Delta H = 333.5$ J g^{-1} = 6.008 kJ mol^{-1}, which is about twice that ($\Delta H = 3.18$ kJ mol^{-1}) of LaMnO$_3$ at T_{JT}. The analogy is expected to be limited only. However, it is curious that the temperature variation of the density of LaMnO$_3$ (Fig. 6) shows some qualitative similarity to that of ice, keeping in mind that the volume contraction at T_{JT} in LaMnO$_3$ is only 0.36% whereas that at the melting of ice is about 8%, more than an order of magnitude higher. It is to be noted that the resistivity of LaMnO$_3$, which decreases with increasing temperature, shows a precursor effect and then drops abruptly at T_{JT} by more than an order of magnitude[7,11] in a way which mimics the temperature variation of the volume (Fig. 4). The drop in resistivity indicates that the e_g electrons become delocalized[7] above T_{JT}. It is interesting to consider whether electron delocalization is assisted by the volume contraction at T_{JT} through the modification of the electronic structure.

In conclusion we have found a volume contraction of LaMnO$_3$ at the orbital order-disorder transition or the melting temperature $T_{JT} \approx 750$ K, and have proposed a qualitative explanation of this unusual phenomenon based on the excess volume needed for the packing of the static distorted octahedra below T_{JT}.

[1] See, for a review, Y. Tokura and N. Nagaosa, Science **288**, 462 (2000), and references therein.

[2] *Colossal Magnetoresistive Oxides*, edited by Y. Tokura (Gordon and Breach, New York, 2000).

[3] E.O. Wollan and W.C. Koehler, Phys. Rev. **100**, 545 (1955).

[4] J.B. Goodenough, Phys. Rev. B **100**, 564 (1955).

[5] J. Kanamori, J. Appl. Phys. **31**, 145 (1961); A.J. Millis, Phys. Rev. B **53**, 8434 (1996); S. Ishihara, J. Inoue, and S. Maekawa, *ibid.* **55**, 8280 (1997); S. Okamoto, S. Ishihara, and S. Maekawa, *ibid.* **65**, 144403 (2002); L.F. Feiner and A.M. Olés, *ibid.* **59**, 3295 (1999); J. Bala and A.M. Olés, *ibid.* **62**, R6085 (2000); J.E. Medvedeva *et al.*, *ibid.* **65**, 172413 (2002).

[6] J. Rodriguez-Carvajal *et al.*, Phys. Rev. B **57**, R3189 (1998).

[7] J.-S. Zhou and J.B. Goodenough, Phys. Rev. B **60**, R15 002 (1999).

[8] Y.S. Touloukian *et al.*, *Thermal Expansion of Metallic Elements and Alloys* (Plenum Press, New York, 1977).

[9] V.F. Petrenko and R.W. Whitworth, *Physics of Ice* (Oxford University Press, Oxford, 2002).

[10] T. Iida and R.I.L. Guthrie, *Physical Properties of Liquid Metals* (Clarendon Press, Oxford, 1988).

[11] T. Chatterji *et al.*, (unpublished).

[12] M.C. Sánchez *et al.*, Phys. Rev. Lett. **90**, 045503 (2003).

[13] I. Loa *et al.*, Phys. Rev. Lett. **87**, 125501 (2001).

[14] See, for example, R.A. Alberty and R.J. Silbey, *Physical Chemistry*, 2nd ed (Wiley, New York, 1996).